Available online at www.sciencedirect.com
SCIENCE DIRECT®
International Journal of Heat and Mass Transfer 47 (2004) 1233–1246
International Journal of HEAT and MASS TRANSFER
www.elsevier.com/locate/ijhmt

Stability of heat pipes in vapor-dominated systems

Pouya Amili, Yannis C. Yortsos *

Petroleum Engineering Program, Department of Chemical Engineering, University of Southern California, Hedco Building, Room 211, Los Angeles, CA 90089-1211, USA

Received 13 March 2003; received in revised form 10 September 2003

Abstract

We study the linear stability of a two-phase heat pipe zone (vapor–liquid counterflow) in a porous medium, either overlying a superheated vapor zone or underlying a subcooled liquid zone. The effects of gravity, condensation and heat transfer on the stability of a planar base state are analyzed in the linear stability limit. The rate of growth of unstable disturbances is expressed in terms of the wave number of the disturbance, and dimensionless numbers, such as the Rayleigh number and a dimensionless heat flux. As in natural convection under single-phase conditions, a critical Rayleigh number exists, above which the system is conditionally unstable. The critical number takes values different than under single-phase conditions and also depends on the applied heat flux. The results find applications to geothermal systems, to enhanced oil recovery using steam injection, as well as to the conditions of the proposed Yucca Mountain nuclear waste repository. This study complements work of the stability of boiling by Ramesh and Torrance [J. Fluid Mech. 257 (1993) 289].

1. Introduction

Heat pipes are steady-state, vapor–liquid (typically, steam-water), countercurrent flow regimes in porous media driven by the application of heat flux and buoyancy [2]. A heat flux, typically applied at the bottom, results in the evaporation of the liquid-phase, which descends due to buoyancy, and in the return upward flow of vapor, which ascends also due to density differences. This steady-state motion gives rise to enhanced heat transfer by convection. Heat pipes in horizontal systems are also possible, driven by capillarity instead of gravity. A number of geothermal reservoirs are characterized by heat pipe action, including the Geysers [2], and the Larderello, Matsukawa and Kawah Kamjang fields [3].

Heat pipes in homogeneous porous media are characterized by two key features: the temperature is approximately constant, equal to the vapor saturation temperature at the prevailing pressure, and the liquid saturation is also approximately uniform spatially [4]. In theory, the spatial extent of a heat pipe can be infinitely large, under the conditions that the porous medium is homogeneous and that the temperature decrease due to the pressure drop is not significant [5–7]. In practice, viscous, capillary, heat transfer and heterogeneity effects limit the spatial extent, however. For example, in heterogeneous systems, changes in permeability induce saturation changes, driven by both capillary and gravity effects [6], and can lead to the termination of the heat pipe regime. McGuiness [8] explored in detail the factors that constraint the extent of a heat pipe. Although in theory heat pipes have a finite extent, due to the inevitable temperature drop, this extent is effectively infinite, in the context of applications, such as geothermal reservoirs.

For a constant heat flux directed against the gravity vector, there are two possible 1-D steady-states, in the absence of heat conduction or capillary effects. These are determined by the solution of the following equation [4,6,9] (see also schematic of Fig. 1)

* Corresponding author. Tel.: +1-213-8210871; fax: +1-213-740-8493.
E-mail address: yortsos@usc.edu (Y.C. Yortsos).

0017-9310/$ - see front matter © 2003 Elsevier Ltd. All rights reserved.
doi:10.1016/j.ijheatmasstransfer.2003.09.015

Nomenclature

C_p	specific heat
H	thickness of the single-phase region
Ra	Rayleigh number for the vapor phase
S	saturation eigenfunction
T	dimensionless temperature
T_{sat}	saturation temperature
g	gravity acceleration
L_v	latent heat of vaporization
k	permeability of porous medium
k_e	effective thermal conductivity of the porous medium
k_{ri}	relative permeability of phase i
p	dimensionless pressure
q	heat flux at the bottom boundary
s	liquid saturation in two-phase region
t	dimensionless time
x, y	dimensionless horizontal and vertical co-ordinates

Greek symbols

Δ	interface location eigenfunction
Σ	saturation eigenfunction
α	thermal diffusivity
β	thermal expansion coefficient
β_1	ratio of heat capacities for rock and vapor
δ	stationary state interface position
ϕ	porosity
κ	wave number of the disturbance
μ	dynamic viscosity
ν	kinematic viscosity
π	pressure eigenfunction
θ	temperature eigenfunction
ρ	density
σ	rate of growth of the disturbance
ω	dimensionless heat flux

Subscripts and superscripts

cr	critical
l	liquid
min	minimum
v	vapor
0	base state
1	perturbed state
*	dimensional

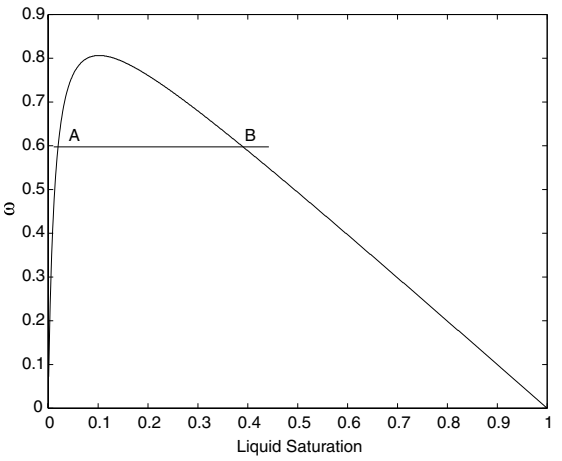

Fig. 1. The two possible steady-state saturations of planar heat pipes (base state). Note the existence of two solutions (if $\omega < \omega_{max} \approx 0.8$) at points A (vapor-dominated) and B (liquid-dominated). If $\omega > \omega_{max}$, a steady-state heat pipe does not develop.

$$\omega \equiv \frac{q\nu_v}{kgL_v(\rho_l - \rho_v)} = \frac{1}{\frac{\nu_l 1}{\nu_v k_{rl}} + \frac{1}{k_{rv}}} \tag{1}$$

Eq. (1) derives from a combination of the steady-state energy and mass balances, under the condition of zero net mass flow. Here, ω is a dimensionless parameter expressing the magnitude q of the applied heat flux, ν is kinematic viscosity, k is permeability, g the acceleration of gravity, L_v the latent heat of vaporization, $k_{ri}(s)$ the relative permeability, a function of the liquid saturation s, and subscripts v and l denote vapor and liquid, respectively. The function in the right-hand side of Eq. (1) vanishes at the two end-points (residual saturations) of the saturation (Fig. 1), at which points the relative permeabilities also vanish.

In graphical terms, the solution of (1) is obtained by the intersection of the heat flux-saturation curve with the horizontal line corresponding to a constant heat flux, ω. Provided that the heat flux is smaller than a critical value, $\omega < \omega_{max}$ (where ω_{max} is equal to about 0.8 in Fig. 1), this results in two solutions (points A and B in Fig. 1). The two different steady-states correspond to a vapor-dominated (VD) or to a liquid-dominated (LD) heat pipe, depending on whether the liquid saturation is small (point A) or large (point B), respectively (see also schematic in Fig. 2). Above the critical value ω_{max}, a heat pipe per se, in the sense of a constant saturation region, is not possible. Instead, a two-phase zone forms of considerably smaller extent and of a monotonically decreasing saturation profile, governed by the competition of capillary and gravity forces (see for example, [6]). We note that in the illustration of Fig. 1, and the results to be presented below, we considered

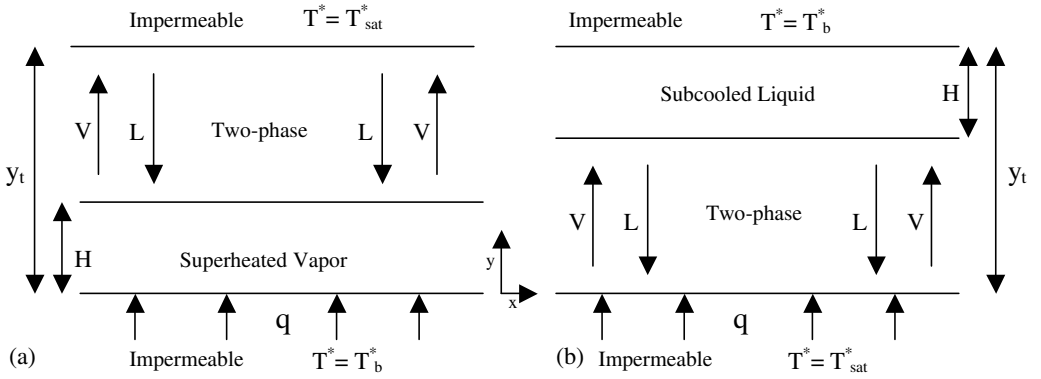

Fig. 2. The two possible steady-state configurations: (a) VD heat pipe (point A in Fig. 1) overlying superheated vapor; (b) LD heat pipe (point B in Fig. 1) underlying subcooled liquid.

straight-line relative permeabilities with zero residual saturations.

Whether of the VD or the LD type, the heat pipe regime is connected to a single-phase flow regime either above or below it. The sequence of regimes in the two configurations (VD or LD) was determined by Stubos et al. [6] by using a small amount of capillarity (which will be neglected here). In applications where the vapor-dominated branch exists, a superheated vapor lies below the two-phase region (Fig. 2a). This situation, often referred to as "dry-out", requires that superheated conditions exist below the two-phase regime. Such an application is possible in geothermal systems, as well as in the high-heat flux scenario for the storage of high-level nuclear waste in the Yucca Mountain repository. In the latter, the high-heat flux generated by the decay of nuclear energy may lead to a dry region surrounding the emplaced waste, overlying which is a steam-water heat pipe driven by the percolating rainwater. Conversely, a liquid-dominated heat pipe develops when (subcooled) liquid layer overlies the heat pipe region (Fig. 2b). Typically, this situation is encountered in boiling at low rates in porous media, where a liquid layer above the two-phase region is maintained, for example by keeping its temperature below boiling [1,10]. Field measurements and observations have confirmed the existence of both VD and LD regimes in geothermal reservoirs. The transition between single-phase and two-phase flow regimes depends on a variety of factors, including the heterogeneity of the medium [6,7,11–13]. We note that while transitions between single-phase and two-phase flow regimes are possible, a transition between the two heat pipe regimes, namely from liquid-dominated to vapor-dominated (B to A) or vice versa (A to B), is not possible [3,6].

Regardless of the particular application, the existence of a heat pipe regime either below an overlying liquid or above an underlying vapor raises questions of gravitational instability. Consider, for example, the case of a liquid-dominated heat pipe. Given that the heat pipe is of a lower (although not by much) density than the overlying liquid, the possibility of a Rayleigh–Taylor gravitational instability arises [14]. The onset of natural convection in the overlying liquid layer, due to its variable temperature, also becomes an important factor. Recall that in porous media, the onset of natural convection under single-phase flow conditions requires that the single-phase Rayleigh number defined as

$$Ra = \frac{kHg\beta\,\Delta T}{\alpha\nu} \tag{2}$$

exceeds a critical value, which for porous media is $Ra_{\min} = 4\pi^2$ [15,16]. Here, H is the thickness of the single-phase region, across which a temperature difference, ΔT, is applied, β is the thermal expansion coefficient and α is the effective thermal diffusivity. The Rayleigh number is a dimensionless number expressing the rate of the destabilizing buoyancy force to the stabilizing viscous force and conductivity.

The stability of liquid-dominated heat pipes was explored by Ramesh and Torrance [1,10] in the context of boiling in porous media. They reported the existence of a critical Rayleigh number above which the 1-D configuration is unstable to 2-D disturbances, and it is a function of the dimensionless heat flux. The minimum critical value reported was about half of that for the onset of natural convection in single-phase flow, suggesting that the underlying two-phase region is destabilizing the flow. As in the single-phase case, stability at large wavelengths was associated with viscous flow, while that at smaller wavelengths was due to conduction. A window of unstable wave numbers was found to exist for Rayleigh numbers larger than the critical. Bau and Torrance [9] conducted boiling experiments in a vertical circular cylinder heated from below and cooled from above. They observed the formation of a

two-phase zone underlying a liquid zone. In the absence of convection, and before the onset of boiling, the temperature profile in the single-phase region was linear, as expected when conduction dominates. After boiling, an almost isothermal region was formed at the saturation temperature, based on which the vertical countercurrent flow of liquid and vapor was concluded. After exceeding a critical Rayleigh number, convection instabilities developed in both phases.

Vapor-dominated heat pipes find applications in similar contexts as liquid-dominated heat pipes. A most interesting visualization was provided recently by Kneafsy and Pruess [17], who studied the mechanisms of heat pipes in a fracture, where superheated conditions were maintained below the two-phase region. Although that study focused mainly on the mechanics of liquid flow, many issues related to flow instability and the possibility that the downwards-percolating liquid may "penetrate" the superheated region, were raised. Pestov [7] examined the stability of the two-phase region (a vapor-dominated heat pipe), which she found to be stable. However, the stability of the combined system, with a vapor-dominated heat pipe overlying a region of an overheated vapor, has not been explored at this time and the stability features of such a configuration are not known. We expect that some of these features should be similar to the liquid-dominated case. For example, we should expect the onset of a natural convection mechanism for the vapor underlying the two-phase region, as well as a gravitational instability due to the two-phase region above being heavier (although only by a small amount) than the underlying vapor. In the context of other problems involving phase change in porous media, for example in steam injection processes for the recovery of heavy oil, condensation of steam at an advancing steam front is less destabilizing, than in non-condensing flows, due to the associated volume reduction. Conversely, the vaporization of liquid is more destabilizing, due to the associated volume expansion. The effect of the phase-transition at the heat pipe interface is unclear, just as it has been unclear for liquid-dominated heat pipes [10].

In this paper, we study the linear stability of vapor-dominated heat pipes by following a linear stability approach, similar to the LD case by Ramesh and Torrance [1,10]. In addition to the base state configuration, other differences exist between our approach and that of Ramesh and Torrance. We consider an infinitely long two-phase zone (heat pipe), as there are no compelling reasons to restrict the two-phase region to a given length. This difference applies also between our work and that of Pestov [7]. The stability analysis is done using analytical methods, which allow for an asymptotic treatment of the problem. As a first approximation, the compressibility of the vapor is not considered, except in driving the natural convection. As reported in [18], a separate analysis that fully accounts for the vapor compressibility did not produce substantial differences. The paper is organized as follows: First, we present a dimensionless formulation of the base state, discuss the properties of the vapor-dominated solution and provide a linearized stability analysis. Results and implications are subsequently discussed. For completeness, the corresponding liquid-dominated configuration is also described.

2. Mathematical formulation

Consider the porous medium configuration shown in the schematic of Fig. 2a. Due to the application of a heat flux, a dry-out region of thickness H, consisting of a superheated vapor of almost constant pressure, P_v^*, ultimately develop at steady-state. Due to heat conduction, this region is of a finite extent, and underlies a two-phase (vapor–liquid) region of (almost) infinite extent. Under stable conditions, the boundary between the two regions is a planar interface, at the saturation temperature T_{sat}^* corresponding to the saturation pressure, P_v^*. Before the onset of convective instabilities, the two-phase region (heat pipe) corresponds to the 1-D vapor-dominated branch of the solution of Eq. (1), assuming that $\omega < \omega_{max}$. At base state conditions, the heat transport is solely by conduction in the vapor zone and by convection in the two-phase zone (vertical counterflow). The temperature profile in the vapor zone is linear due to conductive heat transfer and constant, at the saturation temperature, within the two-phase zone. If convective instability develops, heat transfer in both regions becomes convective. To describe the onset of instability we will first describe the mathematical formulation, then the base state, and finally we will proceed with its stability analysis.

2.1. Governing equations

In the following, in addition to the standard continuum assumptions, the following additional assumptions will be made:

1. The porous medium is uniform, isotropic, fully saturated with fluid, and has constant properties.
2. A conventional multi-phase Darcy description applies.
3. Capillary effects are neglected (see, however, Stubos et al. [6]).
4. The compressibility of the vapor is negligible, except in the buoyancy term, which constitutes a Boussinesq type approximation (see also below).
5. Heat conduction in the two-phase region is negligible, which is thus isothermal at the saturation tempera-

ture of the interface between the vapor and two-phase regions, and of practically infinite extent.

6. The relative permeabilities are linear functions of the liquid saturation.

In the following, asterisks will denote dimensional quantities, and subscripts v, l, and r will represent vapor, liquid, and rock, respectively. The vertical coordinate y points upwards. Based on the above, the following mass, momentum and energy balances can be formulated.

Vapor zone

$$\frac{\partial(\phi\rho_{\mathrm{v}}^*)}{\partial t^*} + \nabla^* \cdot (\mathbf{v}_{\mathrm{v}}^* \rho_{\mathrm{v}}^*) = 0 \tag{3}$$

$$\mathbf{v}_{\mathrm{v}}^* = -\frac{k}{\mu_{\mathrm{v}}}(\nabla^* p^* - \rho_{\mathrm{v}}^* \mathrm{g}) \tag{4}$$

$$\phi\rho_{\mathrm{v}}^* \frac{\partial h_{\mathrm{v}}}{\partial t^*} + (1-\phi)\rho_{\mathrm{r}}^* \frac{\partial h_{\mathrm{r}}}{\partial t^*} + \rho_{\mathrm{v}}^* \mathbf{v}_{\mathrm{v}}^* \cdot \nabla^* h_{\mathrm{v}} = k_{\mathrm{e}} \nabla^{*2} T^* \tag{5}$$

where ϕ is porosity, ρ denotes density and $\mathbf{v}$ is velocity and k_{e} is the effective thermal conductivity of the porous medium. Since ϕ and ρ_{v}^* are constant, this further gives:

$$\nabla^* \cdot (\mathbf{v}_{\mathrm{v}}^*) = 0 \tag{6}$$

The enthalpy of the superheated vapor h_{v} is given by:

$$h_{\mathrm{v}} = h_{vs} + \Delta h_s = h_{vs} + C_{pv}(T^* - T_{\mathrm{sat}}^*) \tag{7}$$

Two-phase zone

The corresponding total mass, momentum and energy balances read

$$\frac{\partial}{\partial t^*}(\phi\rho_{\mathrm{v}}^* s_{\mathrm{v}} + \phi\rho_{\mathrm{l}}^* s_{\mathrm{l}}) + \nabla^* \cdot (\mathbf{v}_{\mathrm{v}}^* \rho_{\mathrm{v}}^* + \mathbf{v}_{\mathrm{l}}^* \rho_{\mathrm{l}}^*) = 0 \tag{8}$$

$$\mathbf{v}_{\mathrm{v}}^* = -\frac{k k_{\mathrm{rv}}}{\mu_{\mathrm{v}}}(\nabla^* p^* - \rho_{\mathrm{v}}^* g) \tag{9}$$

$$\mathbf{v}_{\mathrm{l}}^* = -\frac{k k_{\mathrm{rl}}}{\mu_{\mathrm{l}}}(\nabla^* p^* - \rho_{\mathrm{l}}^* g) \tag{10}$$

$$\frac{\partial}{\partial t^*}(\phi(\rho_{\mathrm{v}}^* h_{\mathrm{v}} s_{\mathrm{v}} + \rho_{\mathrm{l}}^* h_{\mathrm{l}} s_{\mathrm{l}}) + (1-\phi)\rho_{\mathrm{r}}^* h_{\mathrm{r}}) + \nabla^* \cdot (\rho_{\mathrm{l}}^* \mathbf{v}_{\mathrm{l}}^* h_{\mathrm{l}} + \rho_{\mathrm{v}}^* \mathbf{v}_{\mathrm{v}}^* h_{\mathrm{v}}) = k_{\mathrm{e}} \nabla^{*2} T^* \tag{11}$$

where s denotes saturation of a fluid phase, namely the volumetric fraction of the pore volume occupied by that phase, and k_{rl} and k_{rv} are taken to be linear functions of the liquid-phase saturation as previously noted, $k_{\mathrm{rl}} = s_{\mathrm{l}}$ and $k_{\mathrm{rv}} = 1 - s_{\mathrm{l}}$. In the above, we have neglected capillary effects. The two regions are further coupled with the following boundary and interface conditions.

Boundary and interface conditions

The bottom boundary is impermeable

$$\mathbf{v}_{\mathrm{v}} \cdot \mathbf{n} = 0 \tag{12}$$

where $\mathbf{n}$ is the unit normal vector, and at constant temperature

$$T^* = T_{\mathrm{b}}^* \tag{13}$$

At the interface between the vapor zone and the two-phase zone ($y = H$) the temperature is at its saturation value

$$T^* = T_{\mathrm{sat}}^* \tag{14}$$

while continuity of mass, energy and momentum leads to the following:

$$(\rho_{\mathrm{v}}^* \mathbf{v}_{\mathrm{v}}^* + \rho_{\mathrm{l}}^* \mathbf{v}_{\mathrm{l}}^*)^+ \cdot \mathbf{n} - (\rho_{\mathrm{v}}^* \mathbf{v}_{\mathrm{v}}^* + \rho_{\mathrm{l}}^* \mathbf{v}_{\mathrm{l}}^*)^- \cdot \mathbf{n} = \left[(\phi\rho_{\mathrm{v}}^* s_{\mathrm{v}} + \phi\rho_{\mathrm{l}}^* s_{\mathrm{l}})^+ - (\phi\rho_{\mathrm{v}}^* s_{\mathrm{v}} + \phi\rho_{\mathrm{l}}^* s_{\mathrm{l}})^-\right] \cdot \mathbf{v}_{\mathrm{i}}^* \cdot \mathbf{n} \tag{15}$$

$$(\rho_{\mathrm{l}}^* \mathbf{v}_{\mathrm{l}}^* h_{\mathrm{l}} + \rho_{\mathrm{v}}^* \mathbf{v}_{\mathrm{v}}^* h_{\mathrm{v}} - k_{\mathrm{e}} \nabla^* T^*)^+ \cdot \mathbf{n} - (\rho_{\mathrm{l}}^* \mathbf{v}_{\mathrm{l}}^* h_{\mathrm{l}} + \rho_{\mathrm{v}}^* \mathbf{v}_{\mathrm{v}}^* h_{\mathrm{v}} - k_{\mathrm{e}} \nabla^* T^*)^- \cdot \mathbf{n} = \left[\phi(\rho_{\mathrm{v}}^* h_{\mathrm{v}} s_{\mathrm{v}} + \rho_{\mathrm{l}}^* h_{\mathrm{l}} s_{\mathrm{l}})^+ - \phi(\rho_{\mathrm{v}}^* h_{\mathrm{v}} s_{\mathrm{v}} + \rho_{\mathrm{l}}^* h_{\mathrm{l}} s_{\mathrm{l}})^-\right] \mathbf{v}_{\mathrm{i}}^* \cdot \mathbf{n} \tag{16}$$

$$p^{*+} = p^{*-} \tag{17}$$

where $\mathbf{v}_{\mathrm{i}}^*$ is the velocity of the interface, and superscripts + and − indicate two-phase and vapor zones. Finally, the top of the heat pipe region (at $y = y_{\mathrm{t}} \to \infty$) is impermeable

$$(\bar{\rho}_{\mathrm{v}} \mathbf{v}_{\mathrm{v}}^* + \mathbf{v}_{\mathrm{l}}^*) \cdot \mathbf{n} = 0 \tag{18}$$

where we defined the density ratio $\bar{\rho}_{\mathrm{v}} \equiv \frac{\rho_{\mathrm{v}}^*}{\rho_{\mathrm{l}}^*}$.

To proceed further, we will recast the equations in dimensionless form (where asterisks are removed), by using the characteristic variables H^2/α_{v}, H, $v_{\mathrm{v}}\alpha_{\mathrm{v}}/k\rho_{\mathrm{vr}}^*$ for time, length and pressure, where we introduced the vapor thermal diffusivity

$$a_{\mathrm{v}} = \frac{k_{\mathrm{e}}}{\rho_{\mathrm{v}}^* C_{pv}}$$

and defining the dimensionless temperature

$$T = \frac{T^* - T_{\mathrm{sat}}^*}{T_{\mathrm{b}}^* - T_{\mathrm{sat}}^*}$$

We then, obtain the dimensionless governing equations:

Vapor zone

$$\nabla \cdot (\mathbf{v}_{\mathrm{v}}) = 0 \tag{19}$$

$$\mathbf{v}_{\mathrm{v}} = -\nabla p + Ra\, T\mathbf{j} \tag{20}$$

$$\beta_1 \frac{\partial T}{\partial t} + \mathbf{v}_{\mathrm{v}} \cdot \nabla T = \nabla^2 T \tag{21}$$

where $\mathbf{j}$ is the upwards pointing unit vector,

Two-phase zone

$$\beta_2 \frac{\partial s}{\partial t} + \nabla \cdot (\bar{\rho}_{\mathrm{v}} \mathbf{v}_{\mathrm{v}} + \mathbf{v}_{\mathrm{l}}) = 0 \tag{22}$$

$$\mathbf{v}_\mathrm{l} = -\frac{k_\mathrm{rl}}{\bar{\mu}_\mathrm{v}}\left(\nabla p + Ra_{2\phi}\frac{1}{\bar{\rho}_\mathrm{v}}\mathbf{j}\right) \tag{23}$$

$$\mathbf{v}_\mathrm{v} = -k_\mathrm{rv}\nabla p \tag{24}$$

$$-\phi\frac{\partial s}{\partial t} + \nabla\cdot(\mathbf{v}_\mathrm{v}) = 0 \tag{25}$$

where, we defined the single-phase Rayleigh number

$$Ra = \frac{kHg\beta_\mathrm{v}(T^*_\mathrm{b} - T^*_\mathrm{sat})}{\alpha_\mathrm{v}\nu_\mathrm{v}}$$

the two-phase Rayleigh number

$$Ra_{2\phi} = \frac{kHg(1-\bar{\rho}_\mathrm{v})}{\alpha_\mathrm{v}\nu_\mathrm{v}}$$

the ratio of heat capacities of vapor and rock

$$\beta_1 = \frac{\phi\rho_\mathrm{v}C_{pv} + (1-\phi)\rho_\mathrm{r}C_{pr}}{\rho_\mathrm{v}C_{pv}}$$

the ratio of liquid and vapor viscosities,

$$\bar{\mu}_\mathrm{v} = \frac{\mu_\mathrm{l}}{\mu_\mathrm{v}}$$

the dimensionless latent heat

$$\lambda = \frac{L_\mathrm{v}}{C_{pv}(T^*_\mathrm{b} - T^*_\mathrm{sat})}$$

and the parameter $\beta_2 = \phi(1-\bar{\rho}_\mathrm{v})$. The above are accompanied by the interface conditions

$$[(v_\mathrm{l}^+ + \bar{\rho}_\mathrm{v}\mathrm{v}_\mathrm{v}^+) - \bar{\rho}_\mathrm{v}\mathrm{v}_\mathrm{v}^- - [\phi s(1-\bar{\rho}_\mathrm{v})]\mathrm{v_i}]\cdot\mathbf{n} = 0 \tag{26}$$

$$[\lambda(\mathrm{v}_\mathrm{v}^+ - \mathrm{v}_\mathrm{v}^-) + (\phi s\lambda)\mathrm{v_i} + \nabla T^-]n = 0 \tag{27}$$

$$\begin{cases} P^+ = P^- \\ T^+ = T^- = 0 \end{cases} \tag{28}$$

by the impermeability to mass at the bottom of the vapor zone ($y = 0$) and at the top of the heat pipe ($y \to \infty$) and by a constant temperature condition, $T = 1$, at $y = 0$. In the above, bracketed quantities indicates the quantity evaluated across the discontinuity, and superscripts + and − indicate two-phase and vapor zones, respectively.

3. Stability analysis

Subsequently, we carried out a linear stability analysis by assuming that all dependent variables are perturbed in the transverse direction, x, and seeking the rates of growth of these disturbances in terms of normal modes. For this, the base state (subscript 0) must first be calculated. It consists of a stagnant, dry-out vapor region of dimensionless thickness 1, where heat transfer is only by conduction,

$$\frac{\mathrm{d}p_0^-}{\mathrm{d}y} = Ra\,T_0 \tag{29}$$

$$T_0 = 1 - y \tag{30}$$

above which lies an infinite two-phase region, where steady-state counterflow occurs,

$$\frac{\mathrm{d}p_0^+}{\mathrm{d}y} = -\frac{-1}{\lambda k_\mathrm{rv}} \tag{31}$$

$$\mathrm{w_{l0}} = -\frac{\bar{\rho}_\mathrm{v}}{\lambda} \quad \text{and} \quad \mathrm{w_{v0}} = -\frac{1}{\lambda} \tag{32}$$

$$T_0 = 0 \tag{33}$$

$$s = s_0 \tag{34}$$

where we defined the mass flux vector $\mathbf{w}_\mathrm{i} = \boldsymbol{\rho}_\mathrm{i}\mathbf{v_i}$. The base state is then perturbed using normal modes.

3.1. The eigenvalue problem

To find the eigenvalue problem we take disturbances of the form

$$\begin{aligned} T &= T_0 + \varepsilon\theta(y)\exp(\mathrm{i}\kappa\mathrm{x} + \sigma\mathrm{t}) \\ p &= p_0 + \varepsilon\pi(y)\exp(\mathrm{i}\kappa\mathrm{x} + \sigma\mathrm{t}) \\ s &= s_0 + \varepsilon\Sigma(y)\exp(\mathrm{i}\kappa\mathrm{x} + \sigma\mathrm{t}) \\ \delta &= 1 + \varepsilon\Delta\exp(\mathrm{i}\kappa\mathrm{x} + \sigma\mathrm{t}) \end{aligned} \tag{35}$$

where ε is a small parameter, θ, π, Σ, and Δ are the eigenfunctions of temperature, pressure, saturation and interface location, respectively, and κ and σ denote the wave number and the rate of growth of the disturbance. These expansions are then substituted in the governing equations and the boundary conditions, and the system is linearized. The process is detailed, but straightforward. For simplicity, we will present here only the final results, which read as follows:

(a) *Vapor region* (denoted by superscript $^-$ where appropriate) ($0 < y < 1$)

$$\kappa^2\pi^- + Ra\frac{\mathrm{d}\theta}{\mathrm{d}y} - \frac{\mathrm{d}^2\pi^-}{\mathrm{d}y^2} = 0 \tag{36}$$

$$(\beta_1\sigma - Ra + \kappa^2)\theta + \frac{\mathrm{d}\pi^-}{\mathrm{d}y} - \frac{\mathrm{d}^2\theta}{\mathrm{d}y^2} = 0 \tag{37}$$

(b) *Two-phase region* (denoted by superscript $^+$ where appropriate) ($1 < y < \infty$)

$$\kappa^2\pi^+ + \frac{\phi\sigma\bar{\mu}_\mathrm{v}}{k_\mathrm{rl0}}\Sigma - \frac{1}{k_\mathrm{rl0}}\left(\frac{\mathrm{d}p_0^+}{\mathrm{d}y} + \frac{Ra_{2\phi}}{\bar{\rho}_\mathrm{v}}\right)\frac{\mathrm{d}\Sigma}{\mathrm{d}y} - \frac{\mathrm{d}^2\pi^+}{\mathrm{d}y^2} = 0 \tag{38}$$

$$\kappa^2\pi^+ - \frac{\phi\sigma}{k_\mathrm{rv0}}\Sigma + \frac{1}{k_\mathrm{rv0}}\frac{\mathrm{d}p_0^+}{\mathrm{d}y}\frac{\mathrm{d}\Sigma}{\mathrm{d}y} - \frac{\mathrm{d}^2\pi^+}{\mathrm{d}y^2} = 0 \tag{39}$$

The differential equations in these regions are to be solved subject to the following boundary conditions: constant temperature and zero vapor flux at $y = 0$,

$$\begin{cases} \theta = 0 \\ \frac{d\pi^-}{dy} = 0 \end{cases} \tag{40}$$

continuity of mass, energy, temperature and pressure at the interface $y = 1$,

$$\theta = \Delta$$
$$\pi^- - \pi^+ + \frac{\Delta}{\lambda k_{rv0}} = 0$$
$$(\bar{\rho}_v Ra)\theta + (\gamma_1\sigma)\Delta + \left[\frac{1}{\bar{\mu}_v}\left(\frac{dp_0^+}{dy} + \frac{Ra_{2\phi}}{\bar{\rho}_v}\right) - \frac{dp_0^+}{dy}\bar{\rho}_v\right]\Sigma + \left(\frac{k_{rl0}}{\bar{\mu}_v} + \bar{\rho}_v k_{rv0}\right)\frac{d\pi^+}{dy} - \bar{\rho}_v\frac{d\pi^-}{dy} = 0$$
$$(\lambda Ra)\theta - (\gamma_2\sigma)\Delta - \left(\lambda\frac{dp_0^+}{dy}\right)\Sigma - \frac{d\theta}{dy} - \lambda\frac{d\pi^-}{dy} + \lambda k_{rv0}\frac{d\pi^+}{dy} = 0 \tag{41}$$

and no-flux conditions for the vapor and liquid at $y = \infty$,

$$\begin{cases} -k_{rv0}\dfrac{d\pi^+}{dy} + \dfrac{dp_0^+}{dy}\Sigma = 0 \\ -\dfrac{k_{rl0}}{\bar{\mu}_v}\dfrac{d\pi^+}{dy} - \dfrac{1}{\bar{\mu}_v}\left(\dfrac{dp_0^+}{dy} + \dfrac{Ra_{2\phi}}{\bar{\rho}_v}\right)\Sigma = 0 \end{cases} \tag{42}$$

where γ_1 and γ_2 were defined as

$$\begin{cases} \gamma_1 = \phi(1 - \bar{\rho}_v)s_0 \\ \gamma_2 = \phi\lambda s_0 \end{cases} \tag{43}$$

The above equations constitute a fifth-order homogeneous, linear system. We seek the solution for the rate of growth σ as a function of the wave number κ and the various dimensionless parameters, among which key roles are played by the Rayleigh numbers and parameter ω. The solution of the system can be found analytically or numerically, and both approaches will be presented here. The analytical solution assists us to better understand and investigate the asymptotic behavior of the system. It also serves to verify the results of the more flexible numerical approach.

3.2. Analytical solution

Because we have neglected the compressibility of the vapor, the saturation disturbance in the two-phase zone turns out to be zero (in contrast to Pestov [7]). Then, and after several calculations, one can show that the solution of the eigenvalue problem reduces to finding the roots of the determinant of a fourth-order matrix, defined as follows:

$$\mathsf{F}_r = \begin{bmatrix} \tanh(r_1) & \tanh(r_2) & 1 & 0 \\ n_1 & n_2 & \frac{-1}{\lambda k_{rv}} & -1 \\ r_1 n_1 \tanh(r_1) & r_2 n_2 \tanh(r_2) & Ra + \beta_1\sigma\varsigma & c_1\kappa \\ r_1\left(\frac{1}{\lambda} + n_1\tanh(r_1)\right) & r_2\left(\frac{1}{\lambda} + n_2\tanh(r_2)\right) & Ra - \beta_1\sigma\zeta & k_{rv}\kappa \end{bmatrix} \quad \text{if } \kappa^2 + \beta_1\sigma \geqslant Ra \tag{44}$$

$$\mathsf{F}_i = \begin{bmatrix} \tanh(r_1) & \sin(r_3) & 1 & 0 \\ n_1 & n_3 & \frac{-1}{\lambda k_{rv}} & -1 \\ r_1 n_1 \tanh(r_1) & r_3 n_4 & Ra + \beta_1\sigma\varsigma & c_1\kappa \\ r_1\left(\frac{1}{\lambda} + r_1 n_1\tanh(r_1)\right) & r_3 n_4 + \frac{r_3\cos(r_3)}{\lambda} & Ra - \beta_1\sigma\zeta & k_{rv}\kappa \end{bmatrix} \quad \text{if } \kappa^2 + \beta_1\sigma < Ra \tag{45}$$

where the various parameters depend on the wave number, the Rayleigh number and other variables as follows:

$$r_1 = \sqrt{\frac{2\kappa^2 + \beta_1\sigma + \sqrt{(\beta_1\sigma)^2 + 4\kappa^2 Ra}}{2}},$$
$$r_2 = \sqrt{\frac{2\kappa^2 + \beta_1\sigma - \sqrt{(\beta_1\sigma)^2 + 4\kappa^2 Ra}}{2}},$$
$$r_3 = \sqrt{\frac{-2\kappa^2 - \beta_1\sigma + \sqrt{(\beta_1\sigma)^2 + 4\kappa^2 Ra}}{2}},$$
$$n_1 = r_1 - \frac{\beta_1\sigma - Ra + \kappa^2}{r_1},$$
$$n_2 = r_2 - \frac{\beta_1\sigma - Ra + \kappa^2}{r_2},$$
$$n_3 = \left(r_3 + \frac{\beta_1\sigma - Ra + \kappa^2}{r_3}\right)\cos(r_3),$$
$$n_4 = -\left(r_3 + \frac{\beta_1\sigma - Ra + \kappa^2}{r_3}\right)\sin(r_3),$$
$$\varsigma = \frac{\phi(1 - \bar{\rho}_v)s_0}{\bar{\rho}_v\beta_1}, \quad \zeta = \frac{\phi s_0}{\beta_1}, \quad c_1 = \frac{k_{rl0}}{\bar{\rho}_v\bar{\mu}_v} + k_{rv0}$$

It is not difficult to show that the growth constant enters in the combination $\sigma^* = \beta_1\sigma$, and it in this notation that will be reported below.

Vanishing of the determinant of this matrix gives the solution for the rate of growth. The solution procedure is iterative because of the non-linearity of the problem, and for this reason it is done numerically. Direct analytical results are possible in certain cases, however. For

example, in the small wave number limit, $\kappa \ll 1$, one finds after several calculations the following result:

$$\sqrt{-\sigma^*}\tan\left(\sqrt{-\sigma^*}\right) \gg 1$$

This equation admits infinitely many solutions, the largest of which is $\sigma^* = -\pi^2/4$. This prediction will be verified in the numerical results shown below. Conversely, the asymptotic behavior at large wave numbers is

$$\sigma^* \sim -(\text{const})\kappa^2$$

where the positive constant is a function of various parameters. It follows that the system is stable at long and short wavelengths, and conditionally unstable at intermediate values. As discussed in detail below, there exists a critical Rayleigh number, Ra_{crit}, above which the system is unstable in an intermediate range of wave numbers.

3.3. Numerical solution

The system of differential equations (36)–(39) can also be written as a system of first-order ordinary differential equations

$$\frac{d\mathbf{X}_v}{dy} = \mathbf{M}_v\mathbf{X}_v \tag{46}$$

$$\frac{d\mathbf{X}_{2p}}{dy} = \mathbf{M}_{2p}\mathbf{X}_{2p} \tag{47}$$

where

$$\mathbf{X}_v = \begin{bmatrix} \frac{d\pi^-}{dy} \\ \frac{d\theta}{dy} \\ \pi^- \\ \theta \end{bmatrix}, \qquad \mathbf{X}_{2p} = \begin{bmatrix} \frac{d\pi^+}{dy} \\ \pi^+ \\ \Sigma \end{bmatrix}$$

and $\boldsymbol{M}_v$ and $\boldsymbol{M}_{2p}$ are the following matrices:

$$\mathbf{M}_v = \begin{bmatrix} 0 & Ra & \kappa^2 & 0 \\ 1 & 0 & 0 & \beta_1\sigma - Ra + \kappa^2 \\ 1 & 0 & 0 & 0 \\ 0 & 1 & 0 & 0 \end{bmatrix},$$

$$\mathbf{M}_{2p} = \begin{bmatrix} 0 & \kappa^2 & A_6 \\ 1 & 0 & 0 \\ 0 & 0 & A_5 \end{bmatrix} \tag{48}$$

The various coefficients are defined in [18]. The boundary conditions are also recast in matrix form, for example,

$$\text{At } y = 0: \quad \mathbf{BC}_1 \times \boldsymbol{X}_v = 0 \tag{49}$$

where, matrix $\mathbf{BC_1}$ is

$$\mathbf{BC}_1 = \begin{bmatrix} 1 & 0 & 0 & 0 \\ 0 & 0 & 0 & 1 \end{bmatrix} \tag{50}$$

and likewise for the other boundary conditions (matrices $\mathbf{BC}_2$ and $\mathbf{BC}_3$, respectively, see [18]). The shooting method described in Davey [19] was used to solve the boundary value problem. For given values of Ra, ω, σ, and κ, the equations are integrated from $y = 0$ to 1 in the vapor region and from $y = 1$ to ∞ in the two-phase region. Initial conditions are orthonormal vectors given by the columns of an identity matrix of the same dimension. The characteristic equation for stability is then obtained as the determinant of the following 14×14 matrix:

$$\mathsf{F}_n(Ra, \omega, \sigma, \kappa) = 0$$

where

$$\mathsf{F}_n = \det \begin{bmatrix} \mathbf{BC}_1 & 0 & 0 & 0 \\ \mathbf{B}_v & -\mathbf{I} & 0 & 0 \\ 0 & \mathbf{BC}_2 & & 0 \\ 0 & 0 & \mathbf{B}_{2p} & -\mathbf{I} \\ 0 & 0 & 0 & \mathbf{BC}_3 \end{bmatrix} \tag{51}$$

Using both the analytical and the numerical solutions, results obtained are discussed and analyzed in the following section.

4. Results

Fig. 3 shows typical results for the dependence of $\sigma^* = \sigma\beta_1$ on κ at a constant heat flux and for a Rayleigh number greater than the critical. As predicted analytically, for small and large wave numbers the system is stable. The intercept at zero wave numbers equals $-\pi^2/4$ as predicted analytically. A window of unstable wave numbers exists for Rayleigh numbers larger than a critical value. As in the LD case, stability at large wavelengths (small κ) is associated with viscous flow, and at small wavelengths with heat conduction. The behavior is qualitatively similar, although here the problem corresponds to the VD case, to the boiling configuration of Ramesh and Torrance [9]. Instability is the result of two effects: (i) Single-phase natural convection in the vapor region, and (ii) the gravitational instability due to the heavier heat pipe zone overlying the lighter vapor zone. In the remainder of this section we will analyze the sensitivity of the results to the various parameters, such as the Rayleigh number and ω, which contains the dimensionless heat flux.

Fig. 4 is a plot of the σ^*–κ relation for different Ra values at a constant ω. As expected, the system becomes more unstable as the Rayleigh number increases, reflecting the destabilization mostly associated with single-phase natural convection. This behavior is very similar to single-phase convection. To isolate the effect of ω, we consider the behavior at a fixed Rayleigh number. The results, shown in Fig. 5, are similar to the previous.

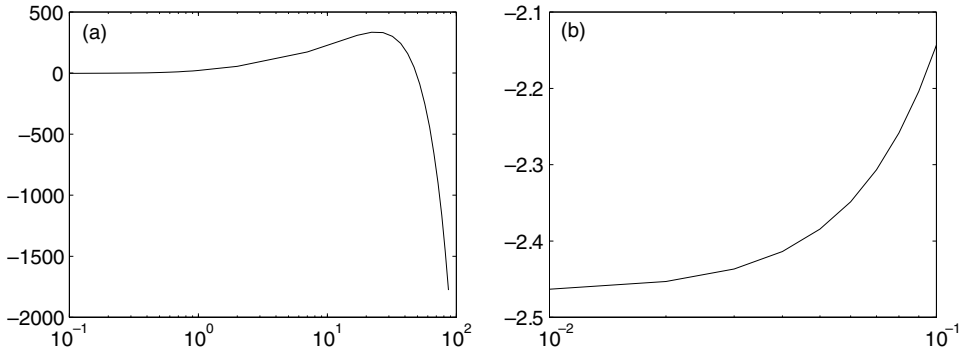

Fig. 3. Typical growth rate-wave number (σ^*–κ) behavior for $Ra > Ra_{crit}$. (a) Over a large range of wave numbers; (b) at small values of the wave number, where the analytical predictions can be tested.

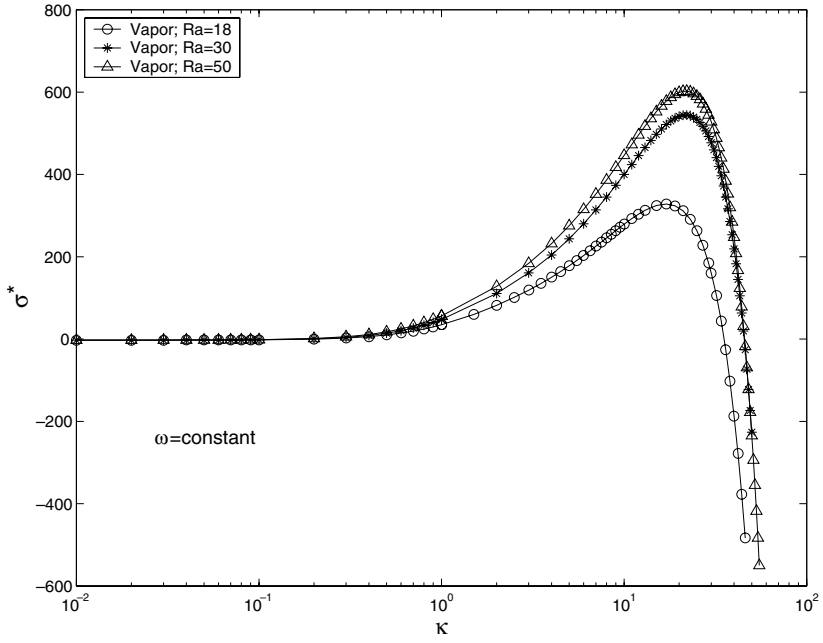

Fig. 4. The σ^*–κ relation for different values of Ra at constant ω for the VD case.

However, the configuration is found to be more unstable, as ω increases. This is primarily a reflection of the gravitational instability, due to the heavier heat pipe overlying the lighter vapor zone. Recall that as ω increases, the liquid saturation in the two-phase zone increases (see also Fig. 1), hence the density contrast increases, resulting in an increase of the tendency for gravitational instability. The figure illustrates the fact that the effect of ω is non-trivial, as it also affects the base state.

The critical Rayleigh number, Ra_{crit}, is a function of the various parameters of the problem, and in particular ω. Fig. 6 shows a plot of Ra_{crit} versus ω assuming a constant latent heat. We find that Ra_{crit} increases as ω decreases, as the system becomes more stable at a lower applied heat flux. The critical value approaches a limiting value close to about 14, at $\omega = 0$. The range of values for Ra_{crit} in this problem is considerably smaller than that corresponding to either single-phase natural convection or to the liquid-dominated problem treated by Ramesh and Torrance [10] (see also below). The dependence of the critical Rayleigh number on ω is a manifestation of the coupling of the heat pipe region with the underlying vapor as well as of the effect of the heat flux in setting the saturation of the heat pipe, and thus the density difference between the two regions. The

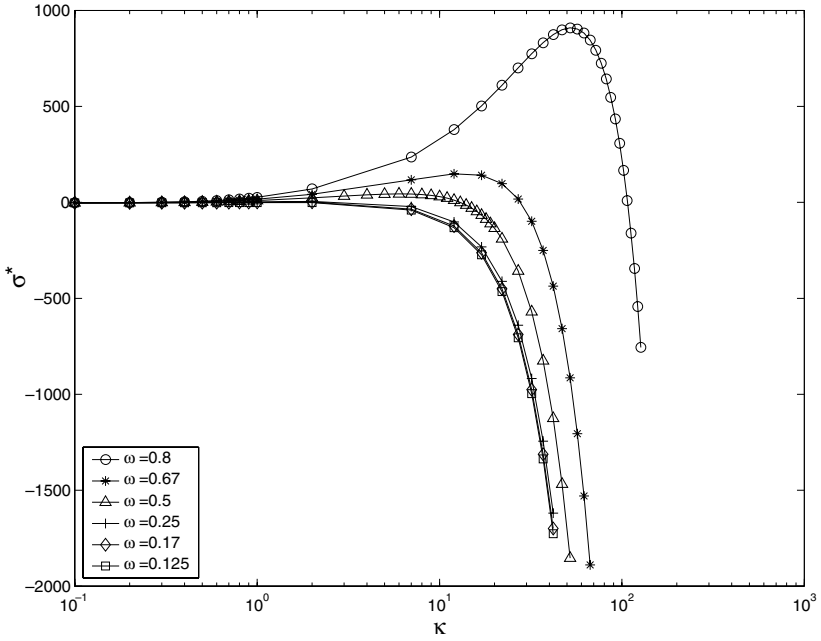

Fig. 5. The σ^*–κ relation for different values of ω at constant Ra for the VD case.

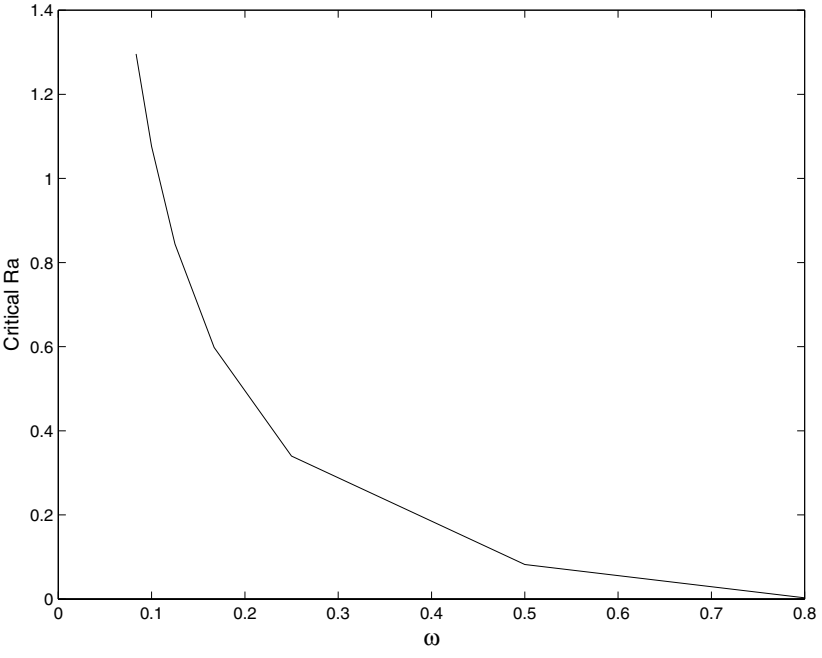

Fig. 6. The dependence of Ra_{crit} on ω for the VD case.

effect of ω on the stability is further discussed below. The effect of the phase change process, and specifically the sensitivity of the results to the latent heat (denoted in the figure as L_V), is shown in Fig. 7, assuming a constant Rayleigh number. We remark that in order to keep a constant Rayleigh number, as the latent heat varies, requires that ω varies in inverse proportion, and the same is true for the velocity of vapor and liquid in

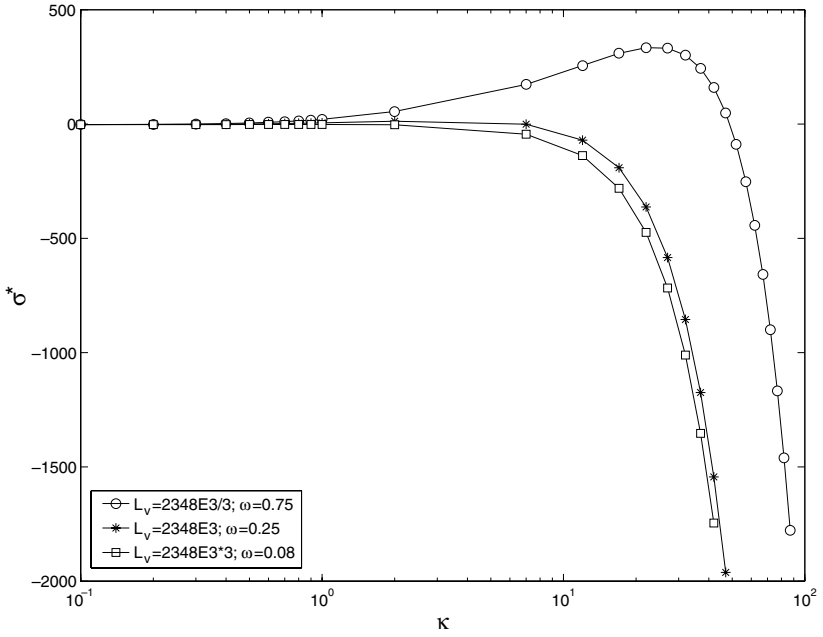

Fig. 7. The effect on stability of the variation of the latent heat (L_v in J/kg) for the VD case.

the two-phase zone. In essence, therefore, this figure reflects the same sensitivity as Fig. 5, which examined the variation of ω. The problem becomes more stable as the latent heat increases, reflecting the higher energy requirements to sustain a destabilizing heat pipe above the vapor region as the latent heat is larger.

4.1. Comparison between vapor-dominated and liquid-dominated heat pipes

A different perspective to our problem can be obtained by comparing the VD case (Fig. 2a) to the LD case (Fig. 2b), where the heat pipe underlies a liquid zone. To obtain a valid comparison between these two cases, we used the same analytical approach, subject to similar boundary conditions as in the vapor-dominated case. Governing equations, boundary conditions and dimensionless parameters for this problem can be found in [18]. The approach is straightforward and will not be repeated. We note that a similar problem was solved by Ramesh and Torrance [1], although our assumptions and configurations are slightly different (for example, we have considered an infinite heat pipe zone, and have also obtained analytical solutions). As previously, small and large κ behaviors are identical to the VD case. Namely, in the small wave number limit, $\kappa \ll 1$, we have

$$\sqrt{-\beta_3\sigma}\tan\left(\sqrt{-\beta_3\sigma}\right) \gg 1$$

where, now,

$$\beta_3 = \frac{\phi\rho_l C_{pl} + (1-\phi)\rho_r C_{pr}}{\rho_l C_{pl}}$$

while at large wave numbers

$$\beta_3\sigma \sim -(\text{const})\kappa^2$$

The relevant growth parameter σ^* is now defined as $\beta_3\sigma$. It follows that the small wave number intercept is still the same, $\sigma^* = -\pi^2/4$.

Fig. 8 shows a comparison between the two cases for the same Rayleigh number and the same value of ω. It is clear that, compared to the VD case, the LD case is unstable at larger wavelengths. The rates of growth σ are of the same order of magnitude, if one notes that the vertical axis in Fig. 8 corresponds to $\beta_1\sigma$ in the VD case and to $\beta_3\sigma$ in the LD case, and also that $\beta_3 \ll \beta_1$. In fact, conversion to this quantity shows that the rate of growth in the LD case is larger than that of the VD case. One important difference between the two cases is the relatively weak dependence on ω in the LD case. The relation between Ra_{crit} and ω for different values of the latent heat is shown in Fig. 9. We note the weaker dependence of the critical value on ω in the LD case, compared to that of the VD case. The trends are also in the opposite direction. Since the two-phase Rayleigh number decreases as ω increases, it can be presumed that the liquid-dominated case is less sensitive than in the vapor-dominated case. However, in the limit $\omega \to 0$, the two cases approach the same value for Ra_{crit}, corresponding

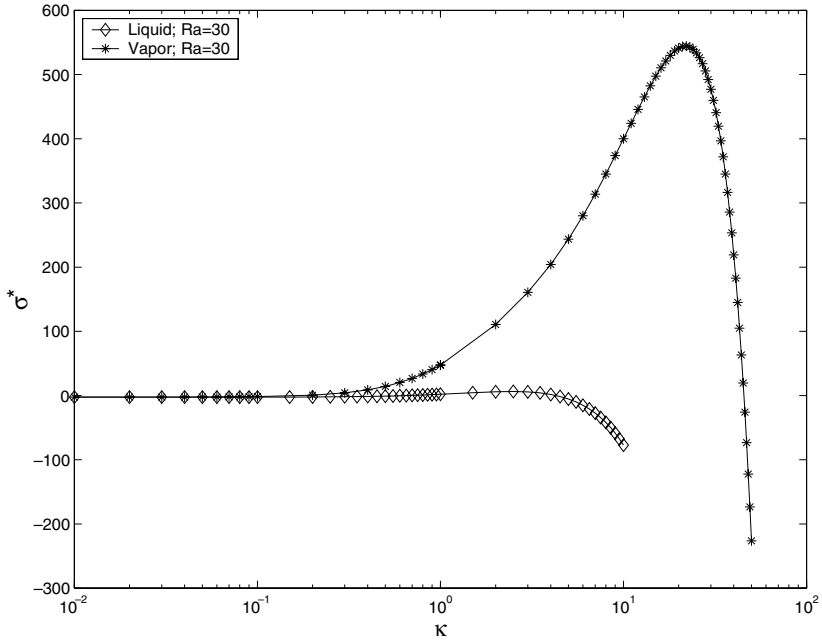

Fig. 8. Comparison between vapor- and liquid-dominated cases at the same value of *Ra*.

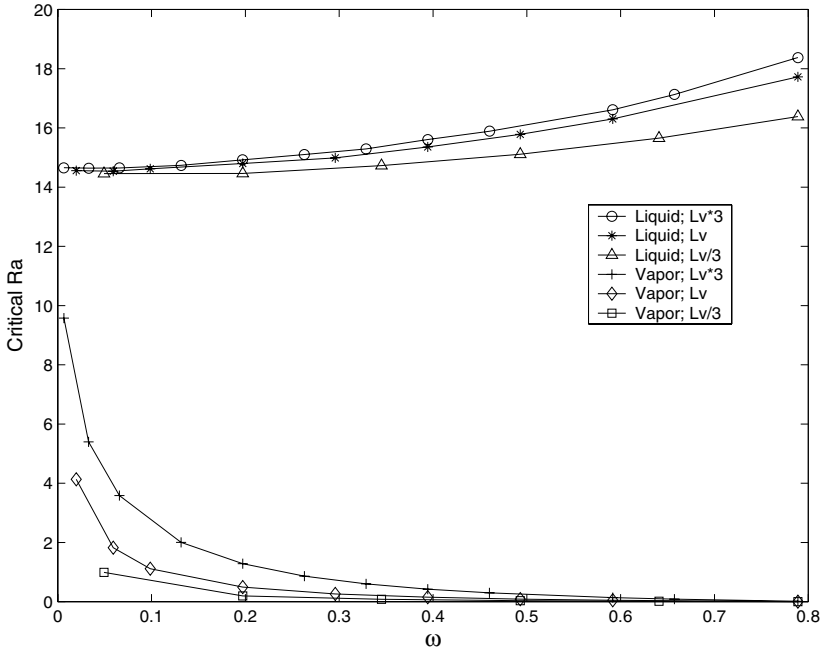

Fig. 9. The dependence of Ra_{crit} on ω for both the LD and the VD cases and for different values of the latent heat ($L_v = 2348.5E3$ J/kg).

to single-phase conditions, as expected. The difference between our results in that limit with the conventional value of $4\pi^2$ [15] is due to the different boundary conditions used here.

The present predictions of heat pipe instability, when the Rayleigh number is sufficiently large, have been experimentally confirmed in a qualitative sense, by the experiments of Kneafsey and Pruess [17] in the VD case

and by Bau and Torrance [9] and Sondergeld and Turcotte [20] in the LD (boiling) case. In these works, significant convective effects were observed when the applied heat flux increased. It is difficult to compare quantitatively our predictions with the experimental findings, as the experimental configuration is more intricate than in the theoretical assumptions (for example in Kneafsey and Pruess [17] the heat flux at the bottom is applied non-uniformly, the heat pipe developing is not infinite, the system contains heat losses, etc.). We also note that our predictions are not identical to those of Pestov [7]. The latter work analyzes a conceptually different problem, namely one in which the two-phase zone is uncoupled from the vapor zone. While presenting a thorough analysis of the two-phase zone, Pestov's work does not really pertain to the present, where the instability is driven by gravity due to the density contrast between the two regimes (heat pipe and vapor).

Our theory predicts the onset of instability in the VD case, when the critical Rayleigh number is of the order of about 1 (see Fig. 6). This means that such configurations are intrinsically more unstable than predicted by single-phase convection alone, namely under otherwise identical conditions, convective instability can develop in reservoirs of permeability of an order of magnitude smaller than for the onset of single-phase convection. The particular permeability values at which instability sets in depend not only on physical parameters (such as density and viscosity) but also on the applied heat flux (namely ω), as well as the thickness of the superheated zone H. This can be readily seen by recasting the Rayleigh number in the form

$$Ra = \left(\frac{kHg}{\alpha_v v_v}\right)^2 \frac{\omega \beta_v L_v \Delta\rho}{\rho_v^* C_{pv}}$$

Vapor compressibility has not been considered up to this point. In order to determine its effect, the entire problem was reformulated and solved by taking into account this parameter. This effort is not being presented here for the sake of brevity, but details can be found in [18]. It was found that in the range of parameters used, the effect of compressibility was not significant, thus it could be safely neglected.

5. Conclusions

In this paper, we studied the linear stability of a two-phase heat pipe zone (vapor–liquid counterflow) in a porous medium, overlying a superheated vapor zone. It was found that the problem has similarities with the liquid-dominated case, in that long and short waves are stable, but intermediate wavelengths can be unstable, depending on the parameter values. A critical Rayleigh number was identified and shown to be different than in natural convection under single-phase conditions in two respects: The critical value is significantly smaller, while it also depends on other parameters of the problem, specifically the heat flux, which controls the base state. The dependence to the latter was found to be considerably stronger in the vapor-dominated case compared to the liquid-dominated case, where the effect was minimal. The results find applications to geothermal systems, to enhanced oil recovery, as well as to the conditions of the proposed Yucca Mountain nuclear waste repository.

Acknowledgements

This research was partly supported by Department of Energy Contract DE-AC26-99BC11521, the contribution of which is gratefully acknowledged.

References

[1] P.S. Ramesh, K.E. Torrance, Boiling in porous layer heated from below: effects of natural convection and a moving liquid/two phase interface, J. Fluid Mech. 257 (1993) 289–309.
[2] D.E. White, L.J. Muffler, A.H. Truesdell, Vapor-dominated hydrothermal systems compared with hot-water systems, Econ. Geol. 66 (1971) 75–97.
[3] M.J. McGuinness, M. Blakeley, K. Pruess, M.J. O'Sullivan, Geothermal heat pipe stability: solution selection by upstreaming and boundary conditions, Transp. Porous Media 11 (1993) 71–100.
[4] K.S. Udell, Heat transfer in porous media considering phase change and capillarity—the heat pipe effect, Int. J. Heat Mass Transfer 28 (1985) 485–495.
[5] C. Satik, M. Parlar, Y.C. Yortsos, A study of steady-state steam-water counterflow in porous media, Int. J. Heat Mass Transfer 34 (1991) 1755–1771.
[6] A.K. Stubos, C. Satik, Y.C. Yortsos, Effects of capillary heterogeneity on vapor–liquid counterflow in porous media, Int. J. Heat Mass Transfer 28 (1993) 485–495.
[7] I. Pestov, Stability of vapor–liquid counterflow in porous media, J. Fluid Mech. 364 (1998) 273–295.
[8] M.J. McGuinness, Geothermal heat pipes—just how long can they be?, Proceedings 15th New Zealand Geothermal Workshop, Auckland, New Zealand, Nov. 1993, 259–266.
[9] H.H. Bau, K.E. Torrance, Boiling in low-permeability porous materials, Int. J. Heat Mass Transfer 25 (1982) 45–54.
[10] P.S. Ramesh, K.E. Torrance, Stability of boiling porous media, Int. J. Heat Mass Transfer 33 (1990) 1895–1908.
[11] M.J. McGuinness, Steady solution selection and existence in geothermal heat pipes-I. The convective case, Int. J. Heat Mass Transfer 39 (1996) 259–274.
[12] M.J. McGuinness, Steady solution selection and existence in geothermal heat pipes-II. The conductive case, Int. J. Heat Mass Transfer 40 (1996) 311–321.
[13] M.J. McGuinness, R. Young, 1-D Geothermal Models—the good, the bad and the unlikely, Proceedings 16th New

Zealand Geothermal Workshop, Auckland, New Zealand, Nov. 1994, 21–28.
[14] P.G. Drazin, W.H. Reid, Hydrodynamic Stability, Cambridge University Press, 1981.
[15] E.R. Lapwood, Proc. Cambridge Philos. Soc. 44 (1948) 508.
[16] B. Gebhart, Y. Jaluria, R. Mahajan, B. Sammakia, Bouyancy-Induced Flows and Transport, Hemisphere Publishing Corporation, 1988.
[17] T.J. Kneafsey, K. Pruess, Laboratory experiments on heat-driven two-phase flows in natural and artificial rock fractures, Water Resources Research 34 (1999) 3349–3367.
[18] P. Amili, Two studies in simultaneous two-phase flow in porous media: I. Heat pipe stability, II. Darcian Dynamics, PhD Thesis, University of Southern California, Los Angeles, CA, 2002.
[19] A. Davey, A simple numerical method for solving Orr-Sommerfeld problems, Q. J. Mech. Appl. Math. 26 (1973) 401.
[20] C.H. Sondergeld, L. Turcotte, An experimental study of two-phase convection in a porous medium with applications to geological problems, J. Geophys. Res. 82 (1977) 2045–2053.